Proceedings of the ASME 2009 Dynamic Systems and Control Conference
DSCC2009
October 12-14, 2009, Hollywood, California, USA

DSCC2009-2729

DERIVATION AND SIMULATION RESULTS OF A HYBRID MODEL PREDICTIVE CONTROL FOR WATER PURGE SCHEDULING IN A FUEL CELL

Giulio Ripaccioli*
Department of Information Engineering
University of Siena
53100, Siena, Italy
Email: ripaccioli@dii.unisi.it

Jason B. Siegel
Anna G. Stefanopoulou
Department or Mechanical Engineering
University of Michigan
Ann Arbor, Michigan, 48109
{siegeljb,annastef}@umich.edu

Stefano Di Cairano
Powertrain Control R&A
Ford Motor Company
Dearborn, Michigan, 48124
dicairano@ieee.org

ABSTRACT

This paper illustrates the application of hybrid modeling and model predictive control techniques to the water purge management in a fuel cell with dead-end anode. The anode water flow dynamics are approximated as a two-mode discrete-time switched affine system that describes the propagation of water inside the gas diffusion layer, the spilling into the channel and consequent filling and plugging the channel. Using this dynamical approximation, a hybrid model predictive controller based on on-line mixed-integer quadratic optimization is tuned, and the effectiveness of the approach is shown through simulations with a high-fidelity model. Then, using an off-line multiparametric optimization procedure, the controller is converted into an equivalent piecewise affine form which is easily implementable even in an embedded controller through a lookup table of affine gains.

1 INTRODUCTION

Water management is a critical issue for PEMFC operation to ensure long stack life and efficient operation. There needs to be sufficient water content in the membrane, (high λ_{mb}), so that proton conduction through the membrane is easy (a dry membrane has higher resistance which leads to voltage loss), but flooding in the channels or catalyst layers is undesirable, and can cause permanent degradation or damage. Water produced at the cathode catalyst layer will diffuse back to the anode side due to the gradient in water concentration across the membrane. During low flows, gravity, buoyancy and channel orientation help establish stratified conditions in the anode channel, which allows for model simplification.

*Address all correspondence to this author.

In the anode channel, water liquid and water vapor will settle to the bottom of the channel and displace hydrogen from that portion of the cell. The impact of channel accumulation is a recoverable reduction in the power output of the fuel cell stack, noticeable from a decrease in cell voltage. When operating with a dead-ended anode, it is necessary to periodically purge the anode channel to remove accumulated inert gas and liquid water [1]. The control input u_b, shown in Fig. 1, can be used to adjust the

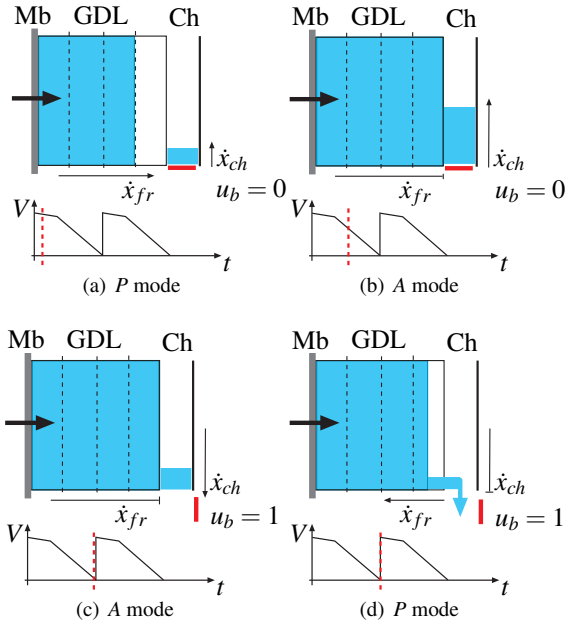

Figure 1. EVOLUTION OF THE WATER ACCUMULATION

purge period and duration. Too frequent purging wastes hydrogen and may over dry the membrane leading to decreased cell performance and other degradation issues. Hence an optimized control of purge-schedule is highly desirable.

The nonlinear PDE model described in [1, 2] is too complex to be used for control design. Thus a simplified discrete-time hybrid dynamical model has been developed in order to design a model based controller.

Hybrid dynamical models have been used in recent years to analyze and optimize a large variety of systems in which physical processes exhibit phase transitions in the form of switches. Several modeling formalisms have been developed to represent hybrid systems [3, 4], including Mixed Logical Dynamical (MLD) systems [5]. MLD is a discrete-time hybrid modeling framework that can be used to formulate optimization problems involving hybrid dynamics. The language HYSDEL (HYbrid Systems DEscription Language) was developed in [6] to obtain MLD models from a high level textual description of the hybrid dynamics. MLD models can be converted into an equivalent piecewise affine (PWA) models [5] through automated procedures [7, 8]. HYSDEL, MLD and PWA models are used in the Hybrid Toolbox for Matlab^{TM} [9] for modeling, simulating, and verifying hybrid dynamical systems and for designing hybrid model predictive controllers.

The water accumulation in a PEMFC can be described as a hybrid automaton with a corresponding discrete-time piecewise affine model. The procedure to obtain the hybrid model from the PDE model involves linearization and time discretization of the important continuous dynamics. Simulated data from the nonlinear equations and real data from neutron imaging [1] have been analyzed to derive the parameters of the PWA model. Once the system is modeled in discrete-time piecewise affine form, it can be implemented as a HYSDEL model. A control-oriented MLD model is generated and used to synthesize the MPC algorithm for the purge management. Finally simulation results for the closed loop system using the high fidelity nonlinear PDE model are presented with guidelines for the selection of weights in the optimization problem. An equivalent explicit form of the control law is also derived, that allows the implementation in a controller hardware with reduced computational resources.

2 HYBRID MODEL FOR CONTROL

The objective of this paper is to design a control law that generates the command for the purge valve u_b based upon the state measurements (or estimates) of liquid water accumulation in the anode GDL and anode channel. This water accumulation is directly related to the fuel cell performance, the cell voltage. The accumulation of liquid water in the channel shown via simulation, is also observed in neutron imaging data [10].

The water propagation and accumulation within the layers of the fuel cell can be characterized by a moving front paradigm, [11, 12] with two linear approximations, for a given set of operating conditions. Hence a natural formulation for the system is as a PWA model.

Our developments are based on a nonlinear model presented in [1]. A ten section discretization ($N = 10$) of the partial differential equations describing reactant and product transport are used here, in order to better resolve the accumulation of liquid water in the Gas Diffusion Layer (GDL) of a PEMFC operating with dead-ended anode. There are two 2nd order diffusion-reaction PDEs describing water transport in the GDL for water vapor and liquid water which are coupled though evaporation and condensation. The dynamics associated with liquid water are much slower than the water vapor gas dynamics, due to the difference in density which is 1000 times greater for liquid. Therefore, when predicting water dynamics and water accumulation in the fuel cell, we can take the gas states to be in steady state [2,12].

The liquid water in the GDL is described in terms of liquid saturation $s = v_l/v_p$, which is the ratio of liquid volume to open pore volume. The steep drop in s at the transition between the liquid and vapor only water areas in the GDL is the result of the sigmoidal function of the capillary pressure and requires very fine discretization of the PDEs [1, 2], in order to accurately represent the front propagation. Therefore, we model the liquid water accumulation in the fuel cell using an ODE moving front approach, similar to [12].

We assume that the liquid water in the GDL is either at a constant volume fraction s_* or zero. The location of the transition from $s = s_*$ to $s = 0$ is called the front location x_{fr} as shown in Fig. 1(a). The constant value s_* at which the liquid water reaches the GDL and then it spreads along the channel (in the flooding case) can be tuned using experimental observations [11].

The nonlinear discretized PDE can be used to extract the normalized liquid water front location, $x_{fr} \in [0, 1]$, in the GDL:

$$x_{fr}(t) = \sum_{i=1}^{N} \frac{s[i]}{s_*} \cdot \frac{1}{N}\,, \tag{1}$$

where $s[i]$ is the liquid water saturation at the ith section of the discretized PDE and N is the number of discretized sections. The GDL front location will be used to derive the first state of the hybrid model. The second state of the hybrid model approximates the accumulation of water in the channel, x_{ch}, as it relates to the PDE model parameter

$$x_{ch}(t) = m_{w,ch}(t) \cdot 10^4, \tag{2}$$

where the mass of water in the channel, $m_{w,ch}$, is scaled by 10^4 in order to improve the numerical stability of the model.

Until the liquid reaches the channel, see Fig. 1(b), the channel accumulation is attributed only to the condensation of the water vapor diffusing from the membrane to the channel through the GDL. Once the water front reaches the channel, the accumulation proceeds with a faster rate due to liquid water flux from the GDL to the channel as shown in Fig. 1(b). When the purge

valve initially opens, liquid water is first removed from the channel shown in Fig. 1(c). Once the liquid water is removed from the channel, then the liquid water front begins to recede back into the GDL Fig. 1(d) moving toward the membrane.

3 Hybrid Automaton

This previously described behavior can be modeled as a linear hybrid automaton [13] with two discrete states. The first discrete state value (P) is associated with the front propagation and recession through the GDL. When the water front reaches the channel, the discrete state switches to the dynamics of water accumulation (A) in the channel. Let $\vartheta \in \{P,A\}$ be the discrete state. The system dynamics are

$$\begin{array}{ll} \text{if } \vartheta(t) = P & \text{if } \vartheta(t) = A \\ \begin{cases} \dot{x_1}(t) = Q_{m2g} - Q_{g2a} \cdot u_b(t) \\ \dot{x_2}(t) = Q_{m2c} \end{cases} & \begin{cases} \dot{x_1}(t) = 0 \\ \dot{x_2}(t) = Q_{g2c} - Q_{c2a} \cdot u_b(t) \end{cases} \end{array} \tag{3}$$

where $x_1(t)$ is the piecewise approximation of the water front position in the GDL, $x_{fr}(t)$, show in (1). The state $x_2(t)$ approximates the mass of water in the anode channel, $x_{ch}(t)$, as shown in (2). Finally, the control input $u_b(t) \in \{0,1\}$ is a boolean variable representing the valve position, where $u_b = 1$ means that valve is open (purging). The normalized water flows from α to β denoted as $Q_{\alpha 2\beta}$ are used to describe the evolution of the two hybrid states. Specifically, the water flow from the membrane to the GDL, Q_{m2g}, is the rate of water accumulation in the GDL which causes the liquid water front propagation inside the GDL. The water flow, Q_{m2c}, due to the condensation of the water vapor transported from the membrane through the GDL to the channel and water flow from the GDL to channel, Q_{g2c}, both lead to water accumulation in the channel. Note that the water accumulation in the channel while the GDL front is moving, Q_{m2c}, is smaller than the water flow from the GDL to the channel when the GDL front reaches the channel, Q_{g2c}. Q_{c2a} is the rate of decrease of water in the channel during the purging phase, while Q_{g2a} is the receding rate of backward movement of the front in the GDL.
The water removal rate from the GDL is a strong function of the pore-size distribution and PTFE coating weight, hence Q_{g2c} and Q_{g2a} depend on the material, as well as on the total flow.

It is then possible to give the transition conditions:

$$\begin{aligned} &\mathrm{P} \rightarrow \mathrm{A} : [x_1 = 1,\ \dot{x_2} \geq 0], \\ &\mathrm{A} \rightarrow \mathrm{P} : [x_2 = 0,\ \dot{x_1} \leq 0], \end{aligned}$$

where the notation $\mathfrak{X} \rightarrow \mathfrak{Y} : [f]$ indicates the state transition from discrete state $\mathfrak{X}$ to discrete state $\mathfrak{Y}$ occurs when the clause of f is true. The invariant sets associated to each discrete states A and P are

$$\begin{aligned} inv(A) &= \{(x_1,x_2) \in \mathbb{R}^2 : x_1 = 1,\ 0 \leq x_2 \leq max_{ch}\}, \\ inv(P) &= \{(x_1,x_2) \in \mathbb{R}^2 : min_{gdl} \leq x_1 \leq 1,\ x_2 \geq 0\}, \end{aligned} \tag{4}$$

where max_{ch} and min_{gdl} are respectively the maximum mass of liquid water that completely fills the channel volume and the minimum position of the front in the GDL.
The parameter identification is performed using simulations of the PDE model [1] and experimental data is described in the following section. Note here that the state x_1, i.e. the level of GDL flooding does not affect the cell voltage because hydrogen can easily diffuse even though a partially flooded GDL. Due to the hydrophobic porous material typically used for GDLs in low temp fuel cells the water will not block all of the pores, hence hydrogen passage to the membrane will not be inhibited until the channel fills with water and blocks hydrogen from entering portions of the GDL.

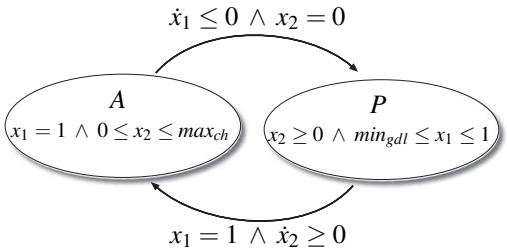

Figure 2. HYBRID AUTOMATON

3.1 DISCRETE TIME PIECEWISE AFFINE SYSTEM

The hybrid automaton (3) can be converted into a piecewise affine (PWA) model [14] and then formulated in discrete time, $x[k] = x(k\,T_s)$, with sampling $T_s = 0.3\ s$. The reformulated PWA system is

$$\begin{array}{l} \text{if } x_1 + x_2 < 1 + \delta_a \qquad \text{(discrete mode P)} \\ \begin{cases} x_1[k+1] = x_1[k] + Q_{m2g}T_s - Q_{g2a}T_s \cdot u_b[k] \\ x_2[k+1] = x_2[k] + Q_{m2c}T_s, \end{cases} \end{array} \tag{5a}$$

$$\begin{array}{l} \text{if } x_1 + x_2 \geq 1 + \delta_a \qquad \text{(discrete mode A)} \\ \begin{cases} x_1[k+1] = x_1[k] \\ x_2[k+1] = x_2[k] + Q_{g2c}T_s - Q_{c2a}T_s \cdot u_b[k], \end{cases} \end{array} \tag{5b}$$

where the switching condition has been changed to improve the numerical stability of the system. To take into account the effect of condensation defined by Q_{m2c} in (3) the transition boundary is increased with a constant $\delta_a \in [0.02 - 0.07]$.
Note that with the formulation in (5) the invariant sets cover $\mathbb{R}^2$, i.e. $\mathcal{S}_{inv}(P) \bigcup \mathcal{S}_{inv}(A) \equiv \mathbb{R}^2$, thus preventing the possibility of the system entering a region where the dynamics are not defined. This problem can arise in practice from numerical integration accuracy or sensor noise.

3.2 Performance Output

Finally we consider the measured output of our system, the fuel cell voltage. Once anode channel flooding occurs, the resulting voltage degradation is associated with the accumulation of liquid water mass in the anode channel, $m_{w,ch}$. Hence the model output is approximated by a linear dependence on x_2:

$$y(t) = v_0 - x_2(t) \cdot v_m, \tag{6}$$

where v_0 is the output voltage of the fuel cell in non-flooding conditions and v_m is a linear gain. Both v_0 and v_m depend on the operating conditions, the load generated I_{fc} in Amperes (A), the fuel cell temperature T in kelvin (K), the cathode air supply ratio λ (unit less), assuming fully humidified cathode inlet, non-humidified anode inlet, and pressure regulated anode conditions as in [1, 15]. We denote the set of operating conditions, $\Omega = [\, I_{fc}, \lambda, T\,]$, that affect the flow rates and the performance output parameters v_0 and v_m.

4 PARAMETER IDENTIFICATION

In order to model the dynamics of the water front in a fuel cell on the anode side as a PWA, the parameter set $\mathbf{Q}(\Omega) = \{Q_{m2g}, Q_{g2a}, Q_{g2c}, Q_{c2a}, Q_{m2c}\}$ which represents the rate of increase and decrease of the water in the different modes, and the voltage parameters $\{v_0, v_m\}$ are identified. These parameters have been obtained by observing simulation data at constant conditions, around several operating points defined by different values for Ω from the nonlinear PDE model, which has been tuned and validated on the experimental data obtained through neutron imaging [15]. Note that the PWA affine model does not continuously depend on the load current. Instead different values of Ω correspond to different parameters and thus different realizations of the PWA model. Tables 1,2 show the parameters as function of the stack current for $T = 333\ (K)$, $\lambda = 2$. The water flow $Q_{g2a} = 0.028$, independent of stack curent. Note that the relation between I_{fc} and the rate of water accumulation is approximately linear. The physically-based nonlinear relationship of $Q(\Omega)$ is being derived in a parallel effort in [11].

I_{fc} (A)	Q_{m2g}/I_{fc} (A^{-1})	Q_{g2c} (10^{-4} kg s^{-1})	Q_{c2a} (10^{-4} kg s^{-1})	Q_{m2c} (10^{-4} kg s^{-1})
10	$1.6 \cdot 10^{-5}$	$4.1 \cdot 10^{-3}$	$4.62 \cdot 10^{-4}$	$3.3 \cdot 10^{-4}$
20	$1.65 \cdot 10^{-5}$	$9.1 \cdot 10^{-3}$	$18.3 \cdot 10^{-4}$	$5.97 \cdot 10^{-4}$
30	$1.7 \cdot 10^{-5}$	$14.1 \cdot 10^{-3}$	$33.7 \cdot 10^{-4}$	$10 \cdot 10^{-4}$

Table 1. MODEL PARAMETERS

The parameters Q_{m2g} and Q_{g2a} have been obtained by the analysis of x_{fr}, from (1), under different conditions for the 53 cm^2 single cell in [15]. Q_{m2g} represents the rate of water

I_{fc} (A)	i_{fc} (A cm^{-2})	v_0 (mV)	v_m ($\frac{mV}{kg}$)
10	0.189	755	$3.5 \cdot 10^{-4}$
20	0.337	618	$5.4 \cdot 10^{-4}$
30	0.566	505	$7.7 \cdot 10^{-4}$

Table 2. VOLTAGE PARAMETERS

front $x_1(t)$ measured in the steeper and initial part after the purge. Q_{g2a} is the rate of water decreasing and it is measured as the difference between $x_1(t) = 1$, front at the channel, and the water front position after the purge over the purge duration. Due to the normalization in (1), Q_{m2g} and Q_{g2a} are dimensionless. To determine Q_{m2c}, Q_{g2c}, Q_{c2a} the mass of liquid water in the channel $m_{w,ch}(t)$ from (2) has been analyzed, Fig.3. The parameters will be in [kg $\cdot 10^{-4}$ s^{-1}] due to the scaling factor introduced in (2). The parameters are determined as

$$Q_{m2c} = \frac{x_2(t_{A_s}) - x_2(t_{\delta_f})}{t_{A_s} - t_{\delta_f}},\ Q_{g2c} = \frac{x_2(t_{\delta_s}) - x_2(t_{A_s})}{t_{\delta_s} - t_{A_s}},\ Q_{g2a} = \frac{x_2(t_{\delta_f}) - x_2(t_{\delta_s})}{t_{\delta_f} - t_{\delta_s}}, \tag{7}$$

where t_{A_s} is the time instant when the accumulation starts and, t_{δ_s}, t_{δ_f} are respectively the initial and final time of the purge.

The parameter v_m in (6) has been determined as

$$v_m = \frac{v(t_2) - v(t_1)}{m_{w,ch}(t_2) - m_{w,ch}(t_1)} \quad \forall (t_1, t_2) \tag{8}$$

while v_0 can be directly calculated by the physics based voltage equation [1]. The value of v_0 is the maximum voltage the fuel cell can supply at a given Ω.

Since we aim to control the purge input $u_b(t)$ as a function of x_1, x_2, y so that the reference commands x_{ref}, y_{ref} are tracked, it is necessary to define the references consistently with the actual operating conditions Ω. The x_{ref} can be set independently from the actual current or temperature as shown in the following sections, however y_{ref} depends on Ω continuously since $y(t)$ is driven by v_0. If our objective is to maintain $y(t)$ at the maximum possible value the reference at the initial time t_0 is $y_{ref} = v_0(t_0)$. In the case of a change in current will occur at time t_1 $v_0(t_1) \neq v_0(t_0)$ and the controller will try to minimize $v_0(t_1) - v_0(t_0)$ which can never converge to zero. To avoid this problem the nonlinear static function $v_0 = f(\Omega)$ has been embedded into a lookup table. Through this function the reference on $y(t)$ is calculated at each sample time. In the following this reference function is called *reference selector*.

5 MLD MODEL VALIDATION

The hybrid dynamical model defined by the the discrete PWA equations (5)-(6) is implemented in HYSDEL. The MLD model obtained using the Hybrid Toolbox for Matlab [9] is

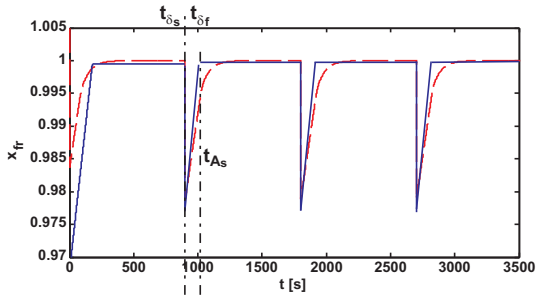

(a) GDL liquid water front (solid line: response of the HYSDEL model, dashed line: response of the nonlinear model, dash-dotted lines: purge event and mode switching event)

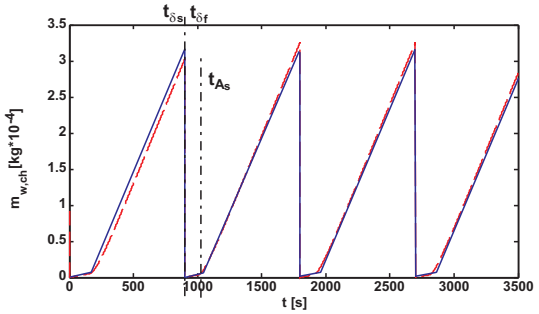

(b) Channel liquid water front (solid line: response of the HYSDEL model, dashed line: response of the nonlinear model, dash-dotted lines: purge event and mode switching event)

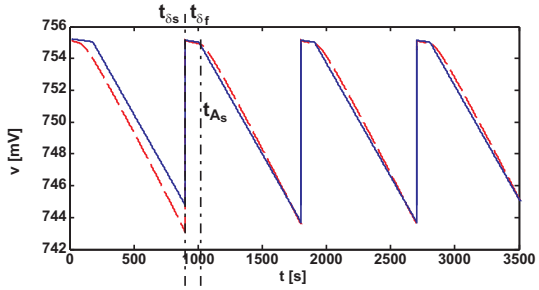

(c) Output voltage (solid line: response of the HYSDEL model, dashed line: response of the nonlinear model, dash-dotted lines: purge event and mode switching event)

Figure 3. MODEL CALIBRATION

equivalent to the piecewise affine (PWA) model [5]. The resulting MLD model, is described by linear dynamic equations subject to linear mixed integer equations, i.e. inequalities containing both continuous and binary variables.

In order to account for modeling errors, constraints on the states of the system, the water front position and the channel water mass accumulation, are included in the modeling framework, to be used for the controller design. These constraints are chosen to be tighter than the limits for safe operation of the physical system:

$$\begin{aligned} min_{gdl} \leq x_1(t) \leq 1, \\ 0 \leq x_2(t) \leq max_{ch}. \end{aligned} \tag{9}$$

Therefore the MLD model realization has 2 continuous states (x_1, x_2), 1 binary input (u_b, the purge signal), 1 output (y), 3 auxiliary variables (1 binary, 2 continuous) and 12 mixed-integer linear inequalities.

The model has been validated by running an open-loop simulation under different constant conditions. Figure 3 reports the states x_1, x_2 and the output y of the discrete time PWA model compared to the same data obtained simulating the full non-linear PDE mode of the fuel cell at $I_{fc} = 10\ A$, $\lambda = 2$, $T = 333\ K$, with purge period $\Delta = 900\ s$ (when $u_b = 0$, i.e. the system is dead-ended) and a purge duration $\delta_p = 0.3\ s$ (when $u_b = 1$). Note that during the initial transient there is some model mismatch, though the error is always under 10%, due to the parameters $\mathbf{Q}$ being identified for steady-state conditions. The quality of the fit is adequate to predict the behavior of the water front even over a long time horizon as well as over a horizon in the range of seconds as required for model predictive control.

6 MPC BASED ON-LINE OPTIMIZATION

MPC has found many industrial applications and it has been successfully applied to hybrid dynamical systems [16–18]. In this section we show how we can derive an MPC controller for the purge management in a fuel cell. In the MPC approach, at each sampling instant a finite horizon open-loop optimization problem is solved, by assuming the current state as the initial condition of the problem. The optimization provides an optimal control sequence, only the first element of which is applied to the hybrid system. This process is iteratively repeated at each subsequent time instant, thereby providing a feedback mechanism for disturbance rejection and reference tracking. The optimal control problem is defined as:

$$\min_{\xi} \left(J(\xi, x(t)) \triangleq Z_\rho \rho^2 + \sum_{k=1}^{H} (x_k - x_{ref})^T S (x_k - x_{ref}) + \right. \tag{10a}$$
$$\left. + \sum_{k=0}^{H-1} (u_k - u_{ref})^T R (u_k - u_{ref}) + (y_k - y_{ref})^T Z (y_k - y_{ref}) \right),$$

$$\text{subj. to} \begin{cases} x_0 & = [x_{fr}(t), x_{ch}(t)]^T, \\ x_{k+1} & = Ax_k + B_1 u_k + B_3 z_k, \\ y_k & = Cx_k + D_1 u_k + D_3 z_k, \\ E_3 z_k & \leq E_1 u_k + E_4 x_k + E_5, \\ min_{gdl} - \rho & \leq x_1 \leq 1 + \rho, \\ 0 - \rho & \leq x_2 \leq max_{ch} + \rho, \\ \rho \geq 0 \end{cases} \tag{10b}$$

where H is the control horizon, z_k are the auxiliary variables, $x_k = [x_1[k], x_2[k]]^T$ is the state of the MLD system at sampling time k, $\xi \triangleq [u_0^T, \ldots, u_{H-1}^T, z_0^T, \ldots, z_{H-1}^T, \rho]^T \in \mathbb{R}^{3H+1} \times \{0,1\}^{2H}$ is the optimization vector, Z, R and T are weight matrices, and $Z_\rho = 10^5$ is a weight used to enforce the softened version (10b) of a constraint on accumulation. In particular we define the ref-

erence signals used in (10) as

$$y_{ref} \triangleq v_0, \qquad u_{ref} \triangleq 0, \qquad x_{ref} \triangleq [1\ 0]', \tag{11}$$

The minimum distance to which the liquid front is permitted to recede into the GDL, $min_{gdl} = 0.3$, is chosen to prevent over drying the membrane. The maximum liquid water accumulation, $max_{ch} = 20 \cdot 10^{-4}$ kg, is chosen to prevent a large voltage drop due to water accumulation in the channel, since x_2 is related to the voltage by (6). These constraints are treated as soft, and hence can be violated, but at the price of a large increase in cost. In this way, the MPC controller will try to avoid to violate them as much as possible. Soft constraints which are chosen to be more conservative, help account for modeling error and mitigate the risk of damaging the system.

Problem (10) can be transformed into a mixed integer quadratic program (MIQP), i.e., the minimization of a quadratic cost function subject to linear constraints, where some of the variables are binary. Even though this class of problems has exponential complexity, efficient numerical tools for its solution are available [19].

6.1 Switching MPC Controller

Since the MPC is based on a PWA model parameterized for a set of constant conditions, Ω, the performance of the controller degrades away from the nominal values. Since we are using state feedback, the controller is less sensitive to model mismatch, however if the model is completely different, closed-loop dynamics will certainly be unsatisfactory. In our case study the stack current can vary over a wide range of current density $i_{fc} \in [0.09 - 0.94]$ A cm^{-2}, and the parameters $Q(\omega)$ will also vary significantly, hence a stack of controllers based on different PWA models is proposed as depicted in Fig. 4. A switching

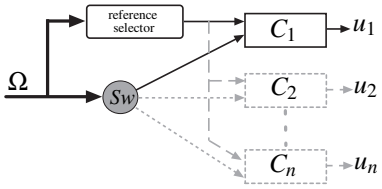

Figure 4. MULTIPLE MPC

entity *Sw* activates a single controller depending on the actual operating conditions $C_i(\Omega(t))$ as well as the reference selector. The complexity in terms of computational time is not affected, because with this structure only the activated controller has to compute the control law at each sample time. The switching strategy implemented in *Sw* and used in simulation, Figure 6, is based on a threshold of current. A more robust switching strategy may be desirable, to avoid chattering phenomena due to noisy signals. A possible solution is based on Kalman filtering coupled with stochastic discrete state estimators [20].

7 SIMULATION RESULTS

The closed-loop behavior of the fuel cell with the MPC controller has been evaluated in simulation by using the high-fidelity nonlinear PDE model described in the first Section. The controller designed using MPC (10), depends on the prediction horizon $H = 10$, and weights

$$Z = 1, \qquad R = 1, \qquad S = \begin{bmatrix} 1 & 0 \\ 0 & 1 \end{bmatrix}, \tag{12}$$

for a given PWA model parameterized at $\Omega = [10,\ 2,\ 333]$. In Figure 5, we consider a simulation scenario with a step change in I_{fc} to check the closed loop robustness to a model mismatch and performance around the nominal value of Ω. The reference voltage, $y_{ref} = 755.25$ mV, and the initial conditions for the simulation are $x_1(0) = 1$, $x_2(0) = 1.13$, $y(0) = 749.43$ mV and $u_b(0) = 0$. At time $t = 423$ s the first purge is commanded by the controller. The purge duration is controlled to 0.3 seconds[1]. The voltage is restored to y_{ref}, as shown in Figure 5(b), the anode channel is drained, Figure 5(a), and the waterfront recedes into the GDL. After 692 seconds (Δ_{C_1}), at $t = 1115$ s, a second purge is required, the purge duration is again $\delta = 0.3$ s. At time $t = 1500$ s the stack current changes from 10 A to 15 A, this leads to a sudden decrease of both actual and reference voltage, y and y_{ref}, respectively. At higher current density, the water accumulation and the voltage degradation rate are faster. The controller reacts by commanding purges at $t = 1719$ s and again at $t = 2171$ s, with a shorter period $\Delta = 452$ s. At time $t = 2500$ s the current increases to $I_{fc} = 20$ A and a purge is required. At $t = 2610.3$ s another purge is commanded and again every $\Delta = 110.3$ s. The controller tuned for lower current density is overly conservative at $I_{fc} = 20$, in attempt prevent large voltage drop, the controller utilizes frequent purging at the expense of efficiency due to waisted hydrogen. This problem can be addressed by using switching MPC controller with sub controllers based on the PWA model parameterized at several desired operating conditions.

7.1 Simulation with switching MPC

The second simulation, shown in Figure 6, presents the closed loop performance with a switched MPC controller for two different sets of weights used in the cost function (10). The model inputs for the simulation are exactly the same as shown in Figure 5. The second controller is based on the PWA model parameterized at $\Omega = [20,\ 2,\ 333]$, with the switching threshold set at $I_{fc} = 16$ A. From $t = 0$ to $t = 2500$ the results are the same as the first simulation. At $t = 2500$ the current increases to 20 A and crosses the switching threshold and activating controller C_2. The solid line in Figure 6 represents a realization of the controller, C_{2A}, using the same weights as C_1, (12). By inspection of the solid line in Fig. 6, before and after the load

[1] It will be evident later that $\delta \equiv T_s$, is not changing because the channel is fully purged in one sampling time, hence a faster or adaptive sampling rate is needed to control the water purged from the channel.

change at $t = 2500$ s, we see that the controller C_{2A} allows the same amount of water accumulation as at the lower current density by choosing a shorter purge period. In this case the switched MPC can correctly predict the fast accumulation at higher currents and perform consistently with the tuning parameters.

The second realization of controller C_{2B}, shown as the dotted line in Fig. 6, is computed with horizon $H = 10$, and weights

$$Z_2 = 1e-1, \qquad R_2 = 10, \qquad S_2 = \begin{bmatrix} 1 & 0 \\ 0 & .1 \end{bmatrix}. \qquad (13)$$

We select lower weights on x_2 and on y and a larger weight on u_b to penalize the valve opening. The purpose is to reduce the hydrogen consumption at the expense of voltage and accumulation reference tracking, hence achieving a larger purge period. Although the controller C_{2B} has better hydrogen utilization, it has a lower safety margin in terms of avoiding a low voltage constraint, and could only be used during a highway driving scenario when changes in load current are infrequent.

It took approximately 173.3 s to simulate the first scenario the closed-loop system on a PC Intel Centrino Duo 2.0 GHz with 2GB RAM running the Hybrid Toolbox for Matlab [9] and the MIQP solver CPLEX 9 [19], of which 105.9 s are spent by CPLEX. That is an average of approximately 0.9 ms per time step. Because of the excessive CPU requirements for on-line optimization and because of the complexity of the software for solving the mixed-integer programs, the MPC controller cannot be directly implemented in an embedded micro-controller or in a computer not equipped with optimization software. To circumvent such implementation problems, in the next section we compute an *explicit* version of the MPC controller that does not require on-line mixed-integer optimization.

8 EXPLICIT HYBRID MPC CONTROLLER

Since the MPC controller based on the optimal control problem cannot be directly implemented in a standard embedded micro-controller, as it would require an MIQP to be solved on-line, the design of the controller is performed in two steps. First, the MPC controller is tuned in simulation using MIQP solvers, until the desired performance is achieved. Then, for implementation purposes, the explicit piecewise affine form of the MPC law is computed off-line by using a combination of multiparametric quadratic programming [21] and dynamic programming, and implemented in the Hybrid Toolbox [9]. The value of the resulting piecewise affine control function is identical to the one which would be calculated by the MPC controller (10), but the on-line complexity is reduced to the simple function evaluation instead of on-line optimization.

As shown in [22], the explicit representation $u(t) = f(\theta(t))$ of the MPC law (10) is represented as a collection of affine gains over (possibly overlapping) polyhedral partitions of the set of parameters $\theta = [x_1\ x_2\ y\ x_{1,ref}\ x_{2,ref}\ y_{ref}]'$

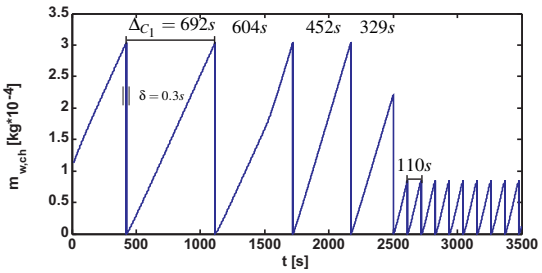

(a) GDL liquid water front

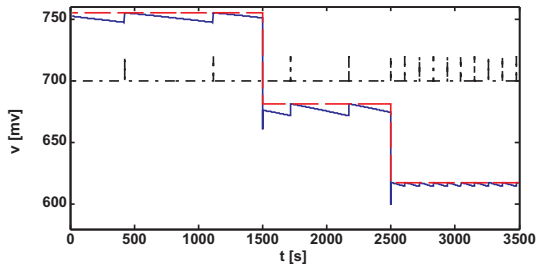

(b) Output voltage (solid line: response of the controller, dashed line: desired value, dash-dotted line: purge signal)

Figure 5. CLOSED-LOOP RESPONSE

For the control horizon $H = 10$ we obtain a piecewise affine control law defined over 11304 polyhedral regions. Reducing the horizon to $H = 3$ and eliminating the constraint on $x_2 \leq max_{ch}$ that is always inactive during our simulation scenarios the number of partition can be reduced to 64. The performance with $H = 3$ is comparable to the performance achieved with a longer horizon. With careful tuning on the weights it is possible to obtain the same results shown in the previous section, but with a total simulation time reduced from 173.3 s to 33.6 s on the same computer platform.

9 CONCLUSIONS AND FUTURE WORK

In this paper we presented a systematic approach to developing a controller for purge management in a fuel cell which combines piecewise affine modeling and hybrid model predictive control. The explicit implementation of the MPC, in the form of a piecewise affine control law computed off-line, obviates the need for on-line optimization altogether and makes the overall approach suitable for implementation in devices with reduced computational resources. This implementation uses a state feedback of the front location in the anode GDL x_{fr} and the water level in the anode channel x_{ch}, hence additional effort is required for the estimation of this information from state FC measurements. The positive results in terms of piecewise affine modeling suggest a possible way to approach the problem with an hybrid observer, for instance based on stochastic hybrid state estimators [20].

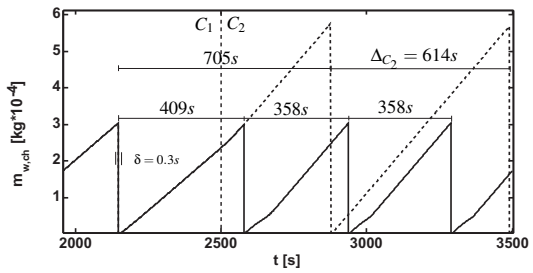

(a) GDL liquid water front

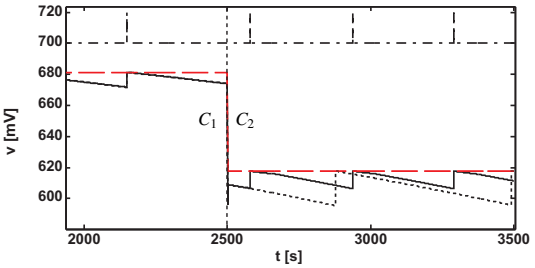

(b) Output voltage (solid line: response of the controller C_{2A} with weights (12), dotted line: response of the controller C_{2B} with weights (13), red dashed line: desired value, dash-dotted line: purge signal)

Figure 6. CLOSED-LOOP RESPONSE: SWITCHING MPC

REFERENCES

[1] McKay, D., Siegel, J., Ott, W., and Stefanopoulou, A., 2008. "Parameterization and prediction of temporal fuel cell voltage behavior during flooding and drying conditions". *Journal of Power Sources*.

[2] McCain, B. A., Stefanopoulou, A. G., and Kolmanovsky, I. V., 2008. "On the dynamics and control of through-plane water distributions in pem fuel cells". *Chemical Engineering Science,* **63**(17), Sept., pp. 4418–4432.

[3] Branicky, M., 1995. "Studies in hybrid systems: modeling, analysis, and control". PhD thesis, LIDS-TH 2304, Massachusetts Institute of Technology, Cambridge, MA.

[4] Heemels, W., Schutter, B. D., and Bemporad, A., 2001. "Equivalence of hybrid dynamical models". *Automatica,* **37**(7), July, pp. 1085–1091.

[5] Bemporad, A., and Morari, M., 1999. "Control of systems integrating logic, dynamics, and constraints". *Automatica,* **35**(3), Mar., pp. 407–427.

[6] Torrisi, F., and Bemporad, A., 2004. "HYSDEL — A tool for generating computational hybrid models". *IEEE Trans. Contr. Systems Technology,* **12**(2), Mar., pp. 235–249.

[7] Bemporad, A., 2004. "Efficient conversion of mixed logical dynamical systems into an equivalent piecewise affine form". *IEEE Trans. Automatic Control,* **49**(5), pp. 832–838.

[8] Geyer, T., Torrisi, F., and Morari, M., 2003. "Efficient Mode Enumeration of Compositional Hybrid Models". In *Hybrid Systems: Computation and Control*, A. Pnueli and O. Maler, eds., Vol. 2623 of *Lecture Notes in Computer Science*. Springer-Verlag, pp. 216–232.

[9] Bemporad, A., 2004. *Hybrid Toolbox – User's Guide*. Jan. `http://www.dii.unisi.it/hybrid/toolbox`.

[10] Siegel, J., McKay, D., Stefanopoulou, A., Hussey, D., and Jacobson, D., 2008. "Measurement of Liquid Water Accumulation in a PEMFC with Dead-Ended Anode". *Journal of The Electrochemical Society,* **155**, p. B1168.

[11] Siegel, J. B., and Stefanopoulou, A. G., 2009. "Through the membrane & along the channel flooding in pemfcs.". In 2009 American Control Conference.

[12] Promislow, K., Chang, P., Haas, H., and Wetton, B., 2008. "Two-phase unit cell model for slow transients in polymer electrolyte membrane fuel cells". *Journal of The Electrochemical Society,* **155**(7), pp. A494–A504.

[13] Henzinger, T., 1996. "The theory of hybrid automata". In Logic in Computer Science. LICS'96. Proceedings., Eleventh Annual IEEE Symposium on, pp. 278–292.

[14] Di Cairano, S., and Bemporad, A., 2006. "An equivalence result between linear hybrid automata and piecewise affine systems.". In Proc. 45th IEEE Conf. on Decision and Control, pp. 2631–2636.

[15] Siegel, J., McKay, D., and Stefanopoulou, A., 2008. "Modeling and Validation of Fuel Cell Water Dynamics using Neutron Imaging". In American Control Conference, 2008, pp. 2573–2578.

[16] Borrelli, F., Bemporad, A., Fodor, M., and Hrovat, D., 2006. "An MPC/hybrid system approach to traction control". *IEEE Trans. Contr. Systems Technology,* **14**(3), May, pp. 541–552.

[17] Ripaccioli, G., Bemporad, A., Assadian, F., Dextreit, C., Di Cairano, S., and Kolmanovsky, I., 2009. "Hybrid modeling, identification, and predictive control: an application to hybrid electric vehicle energy management". In Hybrid System: Computational and Control, 2008.

[18] Giorgetti, N., Ripaccioli, G., Bemporad, A., Kolmanovsky, I., and Hrovat, D., 2006. "Hybrid model predictive control of direct injection stratified charge engines". *IEEE/ASME Transactions on Mechatronics,* **11**(5), pp. 499–506.

[19] ILOG, Inc., 2003. *CPLEX 9.0 User Manual*. Gentilly Cedex, France.

[20] Di Cairano, S., Johansson, K., Bemporad, A., and Murray, R., 2008. "Dynamic network state estimation in networked control systems". In *Hybrid Systems: Computation and Control*, M. Egerstedt and B. Mishra, eds., no. 4981 in Lecture Notes in Computer Science. Springer-Verlag, Berlin Heidelberg, pp. 144–157.

[21] Bemporad, A., Morari, M., Dua, V., and Pistikopoulos, E., 2002. "The explicit linear quadratic regulator for constrained systems". *Automatica,* **38**(1), pp. 3–20.

[22] Borrelli, F., Baotić, M., Bemporad, A., and Morari, M., 2005. "Dynamic programming for constrained optimal control of discrete-time linear hybrid systems". *Automatica,* **41**(10), Oct., pp. 1709–1721.